Mineral speciation determination and quantitative x-ray analysis of struvite family crystals precipitated in wastewater

by Luluk Edahwati

Submission date: 26-Nov-2020 09:09AM (UTC+0700)
Submission ID: 1457304874
File name: rmination_and_quantitative_x-ray_analysis_of_struvite_family.pdf (1.11M)
Word count: 5906
Character count: 30669

Mineral speciation determination and quantitative x-ray analysis of struvite family crystals precipitated in wastewater

L. Edahwati [1,2] , S.Muryanto[2,3], J. Jamari[2], and A. P. Bayuseno [2*]

[(1)] Department of Chemical Engineering, Universitas Pembangunan Nasional "Veteran" Jawa Timur, Surabaya 60294, Indonesia
[(2)] Department of Mechanical Engineering, Diponegoro University, Tembalang Kampus, Semarang 50275, Indonesia
[(3)] Department of Chemical Engineering, UNTAG University, Bendhan Dhuwur Campus, Semarang 50233, Indonesia

Abstract

Mineral speciation of struvite family crystals precipitated in a synthetic wastewater containing Mg^{2+}: $NH^{+}{}_{4}$: PO_3^{-4} (MAP) ions were determined in the study. The pH levels by KOH addition and MAP ratios were set up to be the parameter dependence on struvite family crystals precipitation. The Rietveld analysis of XRPD pattern confirmed a mixed product of struvite, struvite-(K) and newberyite precipitated in the solution at a molar ratio of 1:1:1 and pH 8. Likewise, a relative abundance of struvite and struvite-(K) precipitated, as pH was elevated from 9 to 10. However, as the MAP ratio increased from 1:1:1 to 1:2:1, struvite product reached up almost 99 wt. % at the pH selected in the study. A minor impurity of sylvite was frequently found in all precipitating solids. Struvite family crystals with different size and morphology were also observed. Obviously, the relatively pure struvite was obtained through increasing amounts of NH^{4+} in the solution.

Keywords : Precipitation, MAP molar ratio, pH, Struvite, XRPD Rietveld

*Corresponding author at: the Department of Mechanical Engineering, Diponegoro University, Tembalang Campus, Semarang 50275, Indonesia. Tel: +62-24-7460059; Fax: +62-24-7460059.
E-mail address: apbayuseno@gmail.com

Introduction

Struvite is ammonium magnesium phosphate hexahydrate ($NH_4MgPO_4 \cdot 6H_2O$) which can be precipitated from the wastewater. It is regarded as common scale deposits build up along the walls of pipes and pumps in recirculation streams in municipal effluent treatment plants and flushed agricultural operations. The existing scale can cause technical problems such as blocking the inside diameter of pipes and reduction in efficiency of heat exchangers, and restricting flow in surface aerators [1, 2]. This condition thus increases cost of operating an industry, and is necessary to carry out the regular maintenance for equipment cleaning.

On the other hand, struvite precipitation is a prospective technology for recovery of nitrogen and phosphorus from the wastewater as valuable fertilizer constituents [3, 4] . The wastewater contains higher concentrations of dissolved orthophosphates and/or ammonia and magnesium ions, which are an important factor in the struvite scale formation. Furthermore, struvite and other phosphate minerals can be potentially formed in the biological treatment of the hog wastes [5], poultry wastes [6, 7], wine distillery effluents [8], and biosolids from biological phosphorus removal processes [9,10]. Nowdays, struvite recovery is an important issue in wastewater treatment and thus become a subject of intensive study in a laboratory and field experiments [1].

Further, the remarkable increase in interest for struvite recovery is reflected in the number of peer-reviewed publications such as: (i) benefits of nitrogen and phosphorus recovery from wastewater treatments [11], (ii) controlling the crystal growth using a range of chemical inhibitors and chelating agents [12, 13, 14, 15, 16], and (iii) modeling, planning, economic and environmental evaluation [17, 18].

Struvite has a general chemical formula $X^{+}Y^{2+}PO_4 \cdot nH_2O$, where n= 6-8. It can be formed in the presence of Mg^{2+}, NH^{+4} and PO_3^{-4} ions with 1:1:1 molar ratio according to the equation (with n= 0, 1, and 2, as a function of pH) [1]:

$$Mg^{2+}+NH^{+4}+HnPO_4^{n-3}+6H_2O \rightarrow MgNH_4PO_4 \cdot 6H_2O+nH^{+} \quad (1)$$

The struvite crystallization can occur as a result of alteration in the pH value and the fraction of ionization of each component (e.g., ammonia vs. ammonium ion and Mg^{++} vs. MgO^{+}) [19, 20]. The use of $MgCl_2$ in a base solution (typically NaOH or KOH) without over- or under-dosing magnesium may provide the pH range at ideal value (5 -6.5) [19]. In contrast, the use of MgO and $Mg(OH)_2$ may increase the pH value (6.5 -11) and achieve the MAP molar ratio of equal to 1:1:1, which are favorable for the struvite precipitation [1, 21]. However, the only newberyite ($MgHPO_4 \cdot 3H_2O$) can be precipitated at pH < 6 [22]. Hence, the precipitation of newberyite makes ammonium recovery (nutrient removal) less effective. Conversely, newberyite has better characteristics in solubility, morphology, particle size distribution, the adsorption ability, the adhering ability of different surfaces, electrophorus mobility. These features are needed for controlling the formation of unwanted scaling mineralization in pipes, pumps, and other equipment in wastewater and sludge treatment industry [19].

Instead of newberyite, bobierrite ($Mg_3PO_4 \cdot 28H_2O$) can precipitate with struvite from the solutions containing Mg^{+2} compounds, NH_4^{+} and PO_4^{-3} ions [23, 24, 25, 26]. In the pH range of 6-9, trimagnesium phosphate [$Mg_3(PO_4)_2 \cdot 22H_2O$] and bobierrite may hydrate at very low rate [27]. On the MAP system, there are also new struvite typed compounds as potassium magnesium phosphate hexahydrate ($KMgPO_4 \cdot 6H_2O$) or struvite-(K), and sodium magnesium phosphate heptahydrate ($NaMgPO_4 \cdot 7H_2O$) or struvite-(Na). Struvite-(K) is the potassium analog to struvite in spite of the excess of water molecules [28]. In struvite-(K) and struvite-(Na), the respective K^{+} and Na^{+} cations replace the NH_4+ cations. In view of many

struvite-type minerals, struvite polymorph variety can have important biological, agricultural, and industrial implications [29, 30, 31, 32, 33]. Nevertheless, a relatively little work has been devoted to polymorphism of struvite crystals precipitated from the wastewater, while the polymorphism has technological importance of material properties dependencies such as dissolution kinetic, hardness, density or optical properties of the solid-state structure [34].

Further, detail mineralogical characterization of precipitates is the key factor to optimize the formation of struvite crystals [30, 35]. In particular, the crystallization process in the wastewater seems to be rather complex and there are likely mineralogical differences between two group minerals precipitated: namely magnesium phosphates and magnesium-ammonium phosphates [19]. The above review indicates the importance of characterizing these mineral similarities and differences [11, 30, 35]. Additionally, the mineralogical characterization is required to correlate to the mineral precipitation and the thermodynamic modelling parameters and therefore, to optimize phosphorus removal efficiency and/or to control the formation of unwanted scaling mineralization [36].

The present study was undertaken to examine struvite crystal precipitated from the synthetic wastewater containing $Mg(2+)$, $NH_4(+)$ and $PO_4(3-)$ ions, and to quantify the precipitated crystals. The emphasis of this study was to gain some insight into the mineralogical formation of struvite over pH solutions and variation of MAP molar ratios. The species of precipitated minerals were analyzed by the Rietveld refinement method of X-ray powder diffraction (XRPD) and scanning electron microscopy (SEM) equipped by EDX analysis, respectively.

Materials and Methods

Synthetic wastewater preparation:

In this study, the synthetic wastewater containing the constituent ions of struvite family crystals was prepared by using all chemical reagents (NH_4OH, $MgCl_2$ and H_3PO_4) with analytical grade (Merck, Germany). The synthetic solutions were then prepared by mixing those reagents with aquades in a 500 ml-glass beaker at room temperature. The initial concentrations and molar ratios of five major ions are listed in Table 1.

Table 1: Initial concentrations and molar ratios of five major ions in the synthetic wastewater solutions.

Molar ratio	Mg (mol/l)	NH_4	PO_4	K	Cl
1:1:1	0.873581	0.873581	0.873581	0.873581	1.747162
1:2:1	0.804107	1.608216	0.804107	0.804107	1.608216

Crystallization experiments of struvite:

The crystals were precipitated from stock solutions of $MgCl_2$, NH_4OH, and H_3PO_4 which was diluted in 500 ml flasks so that the MAP molar ratios reached up 1:1:1 and 1:2:1. Struvite crystals were grown using a glass beaker mechanically stirred at 200 rpm and three sets of experiment running were performed in this study. The diluted solutions were then adjusted to pH 8, 9 and 10 by the addition of 1 N KOH (analytical reagent grade) and pH was measured continously using a Beckman 44 pH meter, equipped with an Oakton pH probe. The pH measurement was ended up for 70 min. At the end of each test, the precipitates were filtered immediately through a 0.45 µm paper filter and preserved for subsequent material characterization.

The saturation state of precipitating system was predicted using a saturation index (SI) according to the following equation [16]:

$$SI = \log IAP / Ksp \qquad (2)$$

Where, IAP is the free ionic activities product, and *K*sp is the thermodynamic solubility product of the precipitate phase. If $SI > 0$, the solution is under supersaturated and precipitation occurs spontaneously; If $SI = 0$, the solution is in equilibrium; if $SI < 0$, the solution is under saturated and no precipitation occurs. The calculation of SI for solid and dissolved minerals was conducted using the speciation model of the visual Minteq [37].

Materials characterization:

The scale samples were then examined by SEM on a JEOL (30 SFEG) instrument with EDX system. For SEM analysis, disaggregated loose particles of the samples with different particle sizes below 100 μm were embedded in epoxy on an aluminium sample holder. Finally, the samples were sputtered with carbon.

The XRPD data collection for mineralogical phase identification and subsequent quantitative analysis was performed using Cu-Kα monochromated radiation in a conventional Bragg-Brentano (BB) parafocusing geometry (D5005 SHIMATZU). The scan parameters (5-85 ^{O} 2θ, 0.020 steps, 15 s/step) were recorded. A PC-based search- match program, the MATCH Software was employed for identifying possible crystalline phases of precipitates. The crystalline phase obtained by the extensive search match was subsequently validated by the Rietveld full profile fitting analysis [38, 39, 40]. In this way, the Rietveld refinement of XRPD data was carried out by Fullprof software [41].

The parameters refinements of the XRPD data were: (i) the $2\theta^{O}$ scale zero position, (ii) the polynomial fitting for the background with six coefficients, (iii) the phase scale factors, (iv) the cell parameters, (v) the peak asymmetry and the peak shape functions, (vi) the atomic coordinate and anisotropic temperature factors. The Fullprof program fits the diffraction line widths (FWHM) as a function of tan(θ) using the u-v-w formula of Caglioti et al. [42], while starting values of u, v and w were obtained from the values of the measured quartz. Preferred

orientation of struvite was also refined, while other phases were assumed to be absent in all cases. The obtained values of the cell parameters and the calculated (wt. %) levels of mineralogical phases were calculated by the program [38]. The calculation method can be found in detail elsewhere [43, 44].

Results and Discussion

Effects of pH and molar ratio of struvite precipitation:

Struvite precipitation rates were examined at three pH values (8, 9 and 10) and two different of MAP molar ratios, with three experiments conducted in duplicate for repeatability testing. Typical pH data versus time obtained from the experiments are given in Figures 1a, b. At the initial solution pH of 8, it shows that the precipitation processes decreased slightly over time. Likewise, at pH 9, the precipitation gradually decreased to reach the equilibrium conditions. All pH observed in the present study, the only slight reduction of precipitation over time was noted. The predicted magnesium/magnesium-phosphate complexes by the visual Minteq provided $MgHPO_4$ (aq) and HPO_4^{2-} which were the major ions in this struvite formation. Additionally, the major role of phosphate remaining as $MgPO_4^-$, $MgHPO_4$ (aq), and HPO_4^{2-} may control the pH stability [45].

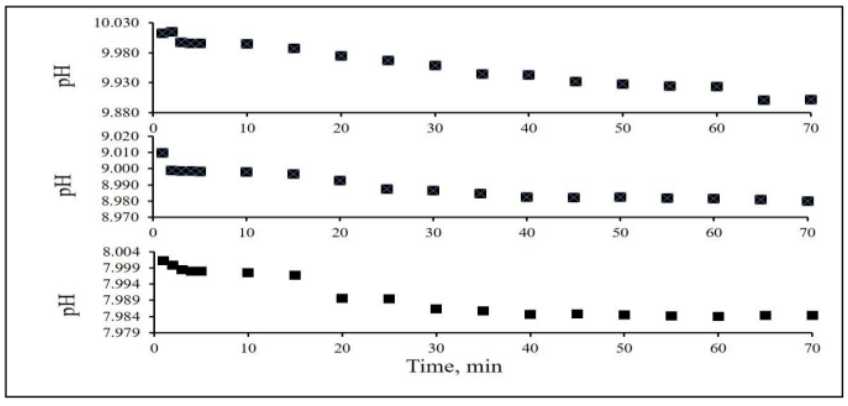

Figure 1a: Measured pH solution over time as the molar ratio of 1: 1: 1 at 30 ^{O}C.

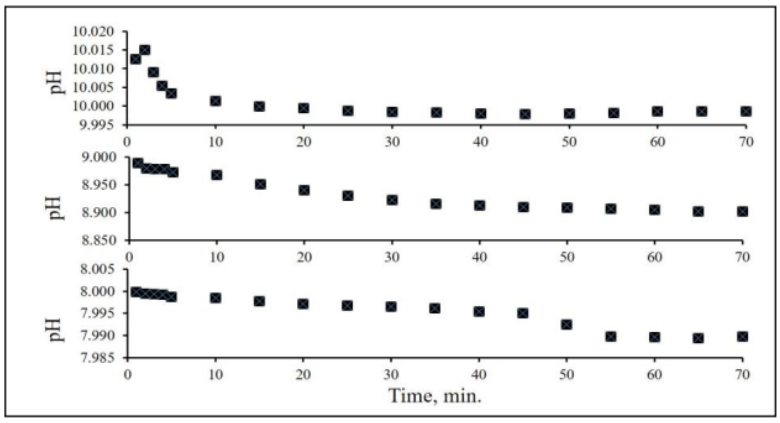

Figure 1b: Measured pH solution over time as the molar ratio of 1: 2: 1 at 30 ^{O}C.

Analysis of crystallization rates was also performed using the pH measured for Mg^{2+} reduction. Here the struvite growth rate was determined through either reduction of (Mg^{2+}) or increase from hydrogen ion, according to the following equation [12, 21]:

$$Ln\ (C\text{-}Ceq) = -kt + Ln\ (C\text{-}C_O) \qquad (4)$$

where C is the concentration of the reactant concentration at a moment t, C_{eq} the reactant concentration at equilibrium, C_O the initial reactant concentration, and k the kinetic constant.

Further, the evolution of the magnesium concentration versus time from the initial pH 8 (Equation-4) is plotted in the same way as in Figure 2. The plots of Ln [$C\text{-}C_{eq}$] versus time for the experimental conditions were initially examined at the MAP molar ratio of 1:1:1 at temperature of 30 ^{O}C. The rate constants obtained from each plot are then presented in Table 2. In the present study, the plots revealed that the calculated Mg concentrations fitted well with the first kinetic order model with a slope of -k, where correlation coefficients (R^2) ranged from 0.957 to 0.975 over the range of initial Mg concentrations examined. As the molar ratio of 1:2:1, good correlations of the magnesium concentration calculated for the first-order kinetic model were also obtained with R^2 values 0.970 to 0.98. The kinetic constants seem to pursue a trend in that the lower the initial pH, the higher the rate constant and therefore the faster the

precipitation. As the molar ratio of 1:1:1, the kinetic constants reduced from 4.62 to 1.52 h^{-1} with increasing pH from 8 to 10. In contrast, at the molar ratio of 1:2:1, the kinetic constants increased from 0.78 to 6.18 h^{-1} since increasing pH from 8 to 10.

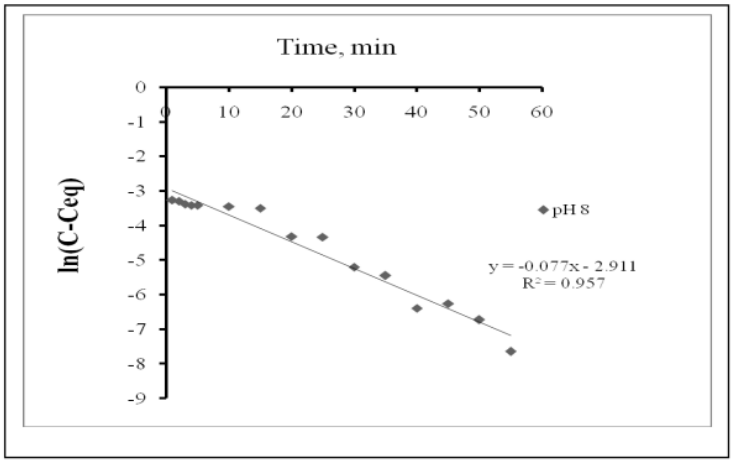

Figure 2: The best fitted straight line through the Ln ($C-C_{eq}$) versus time as the molar ratio of 1:1: 1 at pH of 8 and temperature of 30 ^{O}C.

Table 2: The first order rate constants for struvite crystal growth.

Ratio of 1:1:1, T= 30 ºC, pH	Regression equation	Rate constant, (h^{-1})	R^2
8	Y= -0.077x -2.911	4.62	0.957
9	y= -0.049x – 2.798	2.94	0.968
10	y= -0.026x – 1.196	1.56	0.975
Ratio of 1:2:1, T= 30 ºC, pH			
8	y= -0.013x – 3.757	0.78	0.989
9	y= -0.052x – 3.637	3.12	0.989
10	y= -0.103x – 3.502	6.18	0.970

Further, the use of Mg^{2+} to study the kinetic reactions providing the best fits of the struvite formation of the first-order kinetics was in agreement with the previous finding [10, 12, 21, 46]. The first, second and third-order kinetic models of the struvite precipitation data were also reported by Zhang et al. [10] providing fits with its R-square value of 0.99, 0.93 and 0.79, respectively. In other work, the struvite formation reaction was shown to be fitted well to the first-order kinetics with the rate constants 3.7 h^{-1} at pH 8.4; 7.9 h^{-1} at pH 8.7 and 12.3 h^{-1} at pH

9.0 [21]. In the present study, the calculated rate constant at pH 8 was in agreement with the results of Ohlinger et al. [46], who reported the kinetic reactions fitted with the first-order rate constant of 4.2 h^{-1} at pH 8.3 ($r^2 \geq 0.95$).

Mineral speciation modeling of precipitates:

An evaluation of the possible minerals precipitated from the solution was carried out using the software visual Minteq. The experimental conditions and the mineral speciation results obtained from the calculation are summarized in Table 3. Evidently, the presence of Mg, NH_4, PO_4 and K can be assumed that struvite, struvite-(K) and newberyite were formed. Over the entire pH range (8, 9 and 10) and the MAP molar ratios (1:1:1 and 1:2:1) examined, the mineral speciation analysis yielded that struvite, struvite-(K), newberyite have the positive saturation index (SI) in the solution. Farringtonite [$Mg_3(PO4)_2$] was the only precipitate, that has positive SI, to be removed from the model. This mineral was reported as a slow forming mineral under the experimental setting [27]. Other minerals, notably periclase (MgO), $Mg(OH)_2$ and [$Mg_2(OH)_3Cl{\cdot}4H_2O$], were thermodynamically unstable at this pH observed and would likely to dissolve with time. In the system, sylvite was undersaturated and expected to be not formed. Subsequently, those precipitated minerals obtained from the program was validated by the XRPD method.

Table 3: Mineral species predicted from the visual MINTEQ model.

Mineral species	Solution at T =30 ^{O}C MAP molar ratio of 1:1:1			Solution at T =30 ^{O}C MAP molar ratio of 1:2:1		
	pH 8	pH9	pH10	pH 8	pH9	pH10
	Saturation Index (SI)			Saturation Index (SI)		
Sylvite (KCl)	-2.048	-2.047	-2.041	-2.11	-2.11	-2.107
Periclase (MgO)	-6.848	-4.873	-2.947	-6.871	-4.918	-3.042
$Mg(OH)_2$ (active)	-4.495	-2.519	-0.594	-4.518	-2.565	-0.689
$Mg_2(OH)_3Cl{:}4H_2O$(s)	-5.922	-2.969	-0.113	-6.032	-3.091	-0.332
Farringtonite [$Mg_3(PO_4)_2$]	5.525	7.48	9.191	5.43	7.353	8.994
Newberyite	2.148	2.138	2.03	2.112	2.097	1.979
Struvite	4.890	5.66	5.852	5.126	5.889	6.068
Struvite (K)	1.965	2.953	3.848	1.899	2.881	3.76

Mineralogical characterization of precipitates:

Firstly, the XRPD pattern generated from the sample with the MAP ratio of 1:1:1 and pH 8 matched with the Powder Diffraction Data (PDF#71-2089) for struvite, (PDF#70-2345) for newberyite, (PDF#35-0812) for struvite-(K) and (PDF# 76-3368) for sylvite (*i.e.*, position and intensity of the peaks, Figure 3a). Furthermore, a validation of minerals predicted in the search-match procedure was subsequently made by the full profile Rietveld refinement. Here the overlapped peaks of phases found in the search match or mistakenly assigned phase could be clearly stand out in the difference plots of the calculated and the measured diffraction profile [39, 40, 47]. Therefore, the quality of refinements of the sample can be gauged from the diffraction plot in Figure 3b. The intensity of most peaks is well represented in the calculated diffractogram.

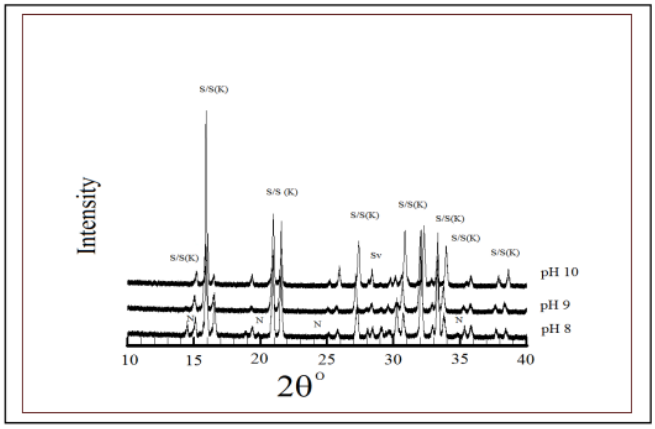

Figure 3a: XRPD difractogram of precipitates obtained from the solution adjusted by pH as the molar ratio of 1: 1: 1 at 30 ^{O}C. The peaks are labelled N (newberyite), S (struvite), S (K) (struvite-K) and Sv (sylvite).

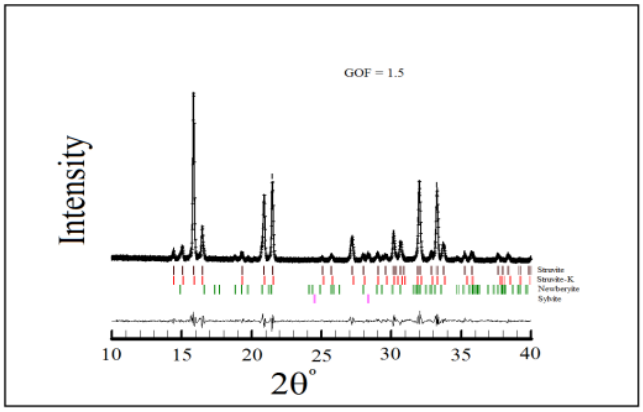

Figure 3b: XRPD Rietveld refinement results for validation of struvite family crystals precipitated at pH 8 as the molar ratio of 1: 1: 1 at 30 ^{O}C. The curves are observed (-------) and calculated (+++++++) patterns respectively; the bottom curve shows the deviation between observed and calculated design. The goodness of fit (GOF) is defined as $GOF^2 = [\sum w_i (y_{io} - y_{ic})^2]/(N-P)$ (where y_{io} and y_{ic} are the observed and calculated intensity at profile point i, the weight w_i is the reciprocal variance of the observed intensity, N is the number of profile points and P is the number of refined parameters.

The precipitates may be only composed of a crystalline structure without amorphous phases present, as indicated by no background noise in the X-ray diffractograms. As the pH increased

(pH 9-10, Figure 3a), the similar XRPD patterns were also observed, but the peaks of newberyite were absent. In addition, struvite and struvite-(K) crystals were grown by the elevated solution pH from 9 to 10. Additionally, the effect of pH on the crystal growth yielded a crystal with irregular prismatic type morphology, as shown by SEM micrograph (Figure 4a).

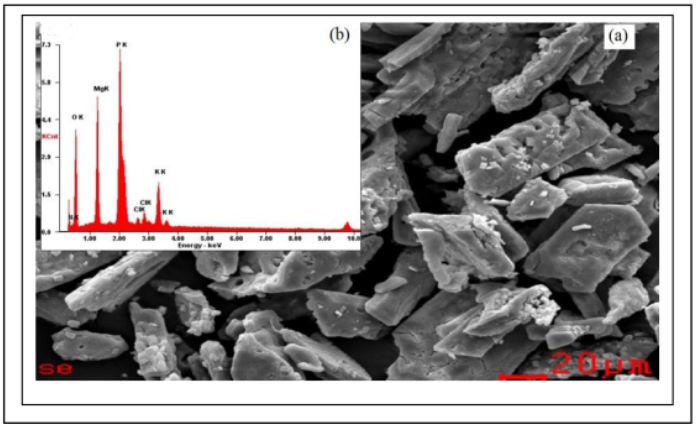

Figure 4: (a) SEM micrograph, (b) EDX analysis of struvite family crystals precipitated from the solution at pH 8 as the molar ratio of 1: 1: 1 at 30 ^{O}C.

In the present study, the crystallization of struvite-(K) was found within the pH range of 8-10 and in the presence of excess potassium. To identify the elemental composition of the minerals, energy dispersive spectrometry (EDX) had been used on specific area localized on the SEM pictures. As expected for samples, the EDX spectrum (Figure 4b) shows that the highest peaks are elements of K, Mg, P and O composing struvite and struvite-(K), in addition to elements Cl for sylvite. Although sylvite was predicted undersaturated in the solution, it could be formed into drying sample.

As the MAP molar ratio increased from 1:1:1 to 1:2:1, the only struvite could be identified in the X-ray diffractograms (Figure 5). As seen from the SEM image, a rod-type morphology is commonly found as struvite crystal (Figure 6a) [48, 49]. The EDX analysis confirmed the highest peaks of Mg, P and O composing struvite, in addition to elements of K and

Cl (Figure 6b). The visual Minteq predicted that struvite (K) and newberyite should be present. Nevertheless, those mineral species may be unstable at this pH observed and would likely to dissolve with time [23, 24, 25, 34].

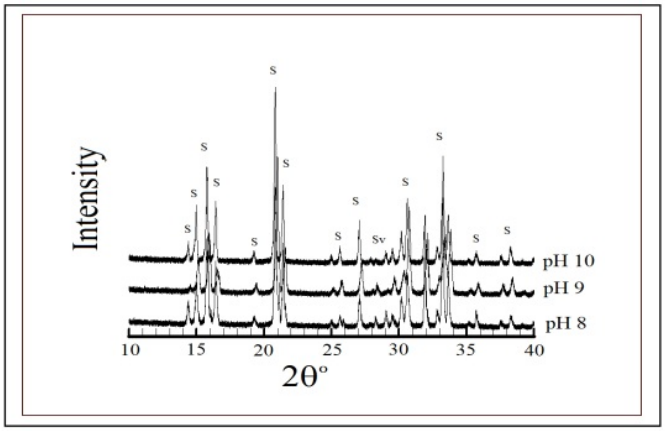

Figure 5: XRPD difractogram of precipitates obtained from the solution adjusted by pH as the molar ratio of 1: 2: 1 at 30 ^{O}C. The peaks are labelled S (struvite), and Sv (sylvite).

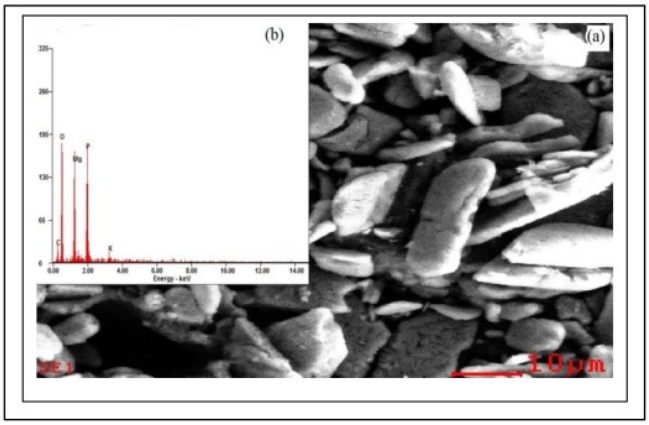

Figure 6: a) SEM micrograph, and b) EDX analysis of struvite crystals precipitated from the solution at pH 8 as the molar ratio of 1: 2: 1 at 30 ^{O}C.

As the molar ratio of 1:2:1 and pH increased from 9 to 10, both of struvite and sylvite peaks could be identified in the X-Ray diffractogram. Similarly, the SEM micrograph showing a rod-type morphology is typically struvite crystals. The crystal growth of rod-like shapes may be

due to the increase in SI for struvite in the solution [48, 49]. Here pH is the controlling parameter on struvite crystal growth and aggregation. The increasing pH levels may be accompanied by an elevating SI solution (Table 3). This condition made the crystal morphology change from a needle shaped to rod shape, as shown in Fig. 6a. The similar finding on the alteration of crystal morphology in struvite has been also reported [49, 50]. Such crystal morphology changes may be related to the degree of crystallinity. The relatively higher SI levels can be also reached at the lower pH values and this condition made the enhanced adsorption for the opposite crystalline phases. Consequently, the crystallization can promote in the other orientation and change in a needle-shaped crystals [51]. In contrast, the rod-shaped habits may occur at the higher pH values with low SI conditions [49, 50]. In particularly, struvite particles are more likely to crystallize into the needle or rod shapes, because they have the orthorhombic structure, while the aggregate forms of the corners or edges of the crystals [52].

The quantity of phosphate minerals produced as a function of MAP ratios and pH is presented in Table 4. As the MAP molar ratio of 1:1:1 and pH 8, struvite, struvite-(K) and newbwryite was the major minerals, with their respective weight percent of 71.7, 18.5 and 8.9 respectively. At the same molar ratio, increasing the pH from 9 to 10 yielded to the reduction of struvite product and the increasing amounts of struvite-(K), while newberyite became absent. Sylvite was always found as an impurity. As the MAP molar ratio of 1:2:1 and the pH range of 8 -10, the major product in struvite (99.4 wt.%) and minor in sylvite (< 1 wt.%) were obtained. The increasing amount of NH^{4+} of the solution suggested that minerals other than struvite were present. However, a stoichiometric excess of ammonium would help drive the reaction to form relatively pure struvite [53], while the excess magnesium decreases struvite precipitation [54]. The total percentage of MAP precipitated has been reported to reach up values of 98 % as the molar ratio of 0.2:1:1, whereas the excess ammonium can be highly beneficial to the precipitation of struvite [53]. On the other hand, the higher struvite- (K) precipitation can be

found at the MAP ratio of 0.01:1:1. Nevertheless, the struvite-(K) formation would be absent, as the molar ratio increases [55]. Apparently, the precipitation of struvite in the molar ratio of 1:2:1 and the pH variation made it possible to recycle more than 90% of phosphorus in large crystals of struvite using the reactant of $MgCl_2$.

Table 4: XRPD results on the mineralogical composition of deposits formed from the solutions.

Mineral	Molar ratio 1:1:1			Molar ratio 1:2:1			Referenced crystals structure model
	pH solution			pH solution			
	8	9	10	8	9	10	
Struvite	71.7 (6)*	63.5(9)	51.3 (9)	99.4 (7)	99.3(9)	99.8 (9)	Whitaker and Jeffery [57]
Struvite (K)	18.5 (4)	35.1(9)	47.3 (7)				Graeser et al. [28]
Sylvite	0.8 (1)	1.4(1)	1.4 (1)	0.6(1)	0.7(1)	0.2 (1)	Ott [56]
Newberyite	8.9 (2)						Abbona and Boistelle [46]

*Figures in parentheses indicate the least-squares estimated standard deviation (esd) referring to the least significant figure to left.

Conclusions

It can be concluded that pH and MAP molar ratios controlled precipitation of struvite family crystals from the wastewater. The rate of disappearance of Mg^{2+} in the solutions increased by reducing pH values. The estimated rate constants were 4.62, 2.94 and 1.56 h^{-1} for pH of 8, 9 and 10, respectively, as the constant MAP molar ratio of 1:1:1 and at 30 ^{O}C. The results of struvite precipitation kinetics with the increasing MAP molar ratio (1:2:1) revealed that the rate constants were found to be 0.78, 3.12 and 6.180 h^{-1}, respectively. The experimental works with different pH and MAP molar ratios clearly resulted in a large variety of phosphate minerals. Struvite, struvite-(K) and newberyite where the major minerals crystallized in the solution at pH 8 and the molar ratio of 1:1:1, while newberyite was absent as the pH increased from 9 to 10. The solution with 1:2:1 of MAP molar ratio and pH range of 8-10, providing the

excess of ammonium, which has a strong effect on the struvite precipitation. The small impurity of sylvite was always found in the precipitates.

Acknowledgements

The work was supported by Universitas Pembangunan Nasional "Veteran" Jawa Timur, Surabaya, Indonesia under the PhD research grant programs.

References

1. Le Corre K.S., Valsami-Jones E., Hobbs P., and Parsons S.A., 2009 'Phosphorus recovery from waste water by struvite crystallization: A Review'. Crit. Rev. Environ. Sci. Technol., 39, 433-477.
2. Mohajit X. K.K., Bhattarai K.K., Taiganides E.P., and Yap B.C., 1989 'Struvite deposits in pipes and aerators'. Biol. Wastes, 30, 133-147.
3. Huang H., Xiao D., Zhang Q., and Li Ding L., 2014 'Removal of ammonia from landfill leachate by struvite precipitation with the use of low-cost phosphate and magnesium sources'. J. Environ. Manage., 145, 191-198.
4. Venkatesan A.K., Hamdan A-H.M., Chavez V.M., Brown J.D., and Halden R.U., 2016 'Mass Balance Model for Sustainable Phosphorus Recovery in a US Wastewater Treatment Plant'. J. Enviro. Qual., 45, 84-89.
5. Schuiling R.D., and Andrade A., 1999 'Recovery of Struvite from Calf Manure'. Environ. Technol., 20, 765-768.
6. Manninen A., Kangas J., Linnainmaa M., and Savolainen H., 1989 'Ammonia in finish poultry houses: Effects of litter on ammonia levels and their reduction by technical binding agents'. Am. Ind. Hyg. Assoc. J., 50, 210-215.

7. Tao W., Fattah K.P., and Huchzermeier M.P., 2016. 'Struvite recovery from anaerobically digested dairy manure: A review of application potential and hindrances'. J. Environ. Manage., 169, 46-57.
8. Loewenthal R.E., Kornmuller U.R.C., and Van Heerden E.P., 1994 'Modelling struvite precipitation in anaerobic treatment systems'. Water Sci. Res., 30, 107-116.
9. Fujimoto N., Mizuochi T., and Togami Y., 1991 'Phosphorus fixation in the sludge treatment system of a biological phosphorus removal process'. Water Sci. Technol., 23, 635-640.
10. Zhang T., Ding L., and Ren H., 2009 'Pretreatment of ammonium removal from landfill leachate by chemical precipitation'. J. Hazard. Mater., 166, 911-915.
11. Mulkerrins D., Dobson A.D.W., and Colleran, E., 2004 'Parameters affecting biological phosphate removal from wastewaters'. Environment International, 30, 249-259.
12. Muryanto S., and Bayuseno A.P., 2014 'Influence of Cu^{2+} and Zn^{2+} as additives on crystallization kinetics and morphology of struvite'. Powder Technol., 253, 602-607.
13. Ohlinger K.N., Young T.M., and Schroeder E.D., 1999 'Kinetics effects on preferential struvite accumulation in wastewater'. J. Environ. Eng., 125, 730-737.
14. Song Y., Hahn H.H., and Hoffmann E., 2002 'Effects of solution conditions on the precipitation of phosphate for recovery, a thermodynamic evaluation'. Chemosphere, 48, 1029-1035.
15. Tchobanoglous G., Burton F.L., and Stensel H.D., 2003 'Meltcalf & Eddy, Inc.'s Wastewater Engineering: Treatment, Disposal, and Reuse', 4th Edition. McGraw-Hill, Inc., New York. 1819.
16. Ye Z., Shen Y., Ye X., Zhang Z., Chen S., and Shi J., 2014 'Phosphorus recovery from wastewater by struvite crystallization: Property of aggregates'. J. Environ. Sci., 26, 991-1000.

17. Gaterell M.R., Gay R., Wilson R., Gochin R.J., and Lester J.N., 2000 'An economic and environmental evaluation of the opportunities for substituting phosphorus recovered from wastewater treatment works in existing UK fertiliser markets'. Environ. Technol., 21, 1067-1084.
18. Le Corre K.S., Valsami-Jones E., Hobbs P., Jefferson B., and Parsons S.A., 2007 'Struvite crystallization and recovery using a stainless steel structure as a seed material'. Water Res., 41, 2449-2456.
19. Babić-Ivančić V., Kontrec J., Brečević L., and Kralj D., 2006 'Kinetics of struvite to newberyite transformation in the precipitation system $MgCl_2$-$NH_4H_2PO_4$-NaOH-H_2O'. Water Res., 40 (18), 3447-3455.
20. Hao X.D., Wang C.C., Lang L., and van Loosdrecht M.C., 2008 'Struvite formation, analytical methods and effects of pH and Ca^{2+}'. Water Sci. Technol., 58, 1687-92.
21. Nelson N.O., Mikkelson R.L., and Hesterberg D.L., 2003 'Struvite precipitation in anaerobic swine lagoon liquid: effect of pH and Mg:P ratio and determination of rate constant'. Bioresource Technol., 89, 229-236.
22. Boistelle R., Abbona F., and Lundager Madsen H.E., 1983 'On the transformation of struvite into newberyite in aqueous system'. Phys. Chem. Miner., 9(5), 216-222.
23. Abbona F., Lundager M.H.E., and Boistelle R., 1982 'Crystallization of two magnesium phosphates: struvite and newberyte: effects of pH and concentration'. J. Cryst. Growth, 57(82), 6-14.
24. Abbona F., Lundager M.H.E., and Boistelle R., 1986 'The initial phases of calcium and magnesium phosphates precipitated from solutions of high to medium concentration'. J. Cryst. Growth, 74 (86), 581-590.

25. Abbona F., Lundager M.H.E., and Boistelle R., 1988. 'The final phases of calcium and magnesium phosphates precipitated from solutions of high to medium concentration'. J. Cryst. Growth, 89 (88), 592-602.

26. Takagi S., Mathew M., and Brown W.E., 1986 'Crystal structures of bobierrite and synthetic $Mg_3(PO4)_2 \cdot 8H_2O$'. Am. Mineral., 71, 1229-1233.

27. Mamais D., Pitt P.A., Cheng Y.W., Loiacono J., and Jenkins D., 1994 'Determination of ferricchloride dose to control struvite precipitation in anaerobic sludge digesters'. Water Environ. Res., 66, 912-918.

28. Graeser S., Postl W., Bojar H-P., Berlepsch P., Armbruster T., Raber T., Ettinger K., and Walter F., 2008 'Struvite-(K), $KMgPO_4 \cdot 6H_2O$, the potassium equivalent of struvite a new mineral'. Eur. J. Mineral., 20, 629-633.

29. Chen L., Shen Y., Xie A., Huang F., Zhang W., and Liu S., 2010 'Seed-mediated synthesis of unusual struvite hierarchical superstructures using bacterium'. Cryst. Growth Design, 10 (5), 2073-2082.

30. Doyle J.D., and Parsons S.A., 2002 'Struvite formation, control and recovery'. Water Res., 36(16), 3925-3940.

31. Haferburg G., Kloess G., Schmitz W., and Kothe E., 2008 'Ni-struvite-a new biomineral formed by a nickel resistant streptomyces acidiscabies'. Chemosphere, 72, 517-523.

32. Trobajo C., Salvado M.A., Pertierra P., Alfonso B.F., Blanco J.A., Khainakov S.A., and Garcia J.R., 2007 'Synthesis, structure and magnetic characterization of two phosphate compounds related with the mineral struvite: $KNiPO_4 \cdot 6H_2O$ and $NaNiPO_4 \cdot 7H_2O$'. Z. Anorg. Allg. Chem., 633, 1932-1936.

33. Weil M., 2008. 'The struvite-type compounds $M(Mg(H_2O)_6)(XO_4)$, where M = Rb, Tl and X = P, As'. Crystal Res. Technol., 43, 1286-1291.

34. Chauhan C.K., Vyas P.M., and Joshi M.J., 2011 'Growth and characterization of struvite-K crystals'. Crystal Res. Technol., 46 (2), 187-194.

35. Parsons S.A., and Doyle J.D., 2004 'Struvite scale formation and control'. Water Sci. Technol., 49, 177-182.

36. Lua X., Shih K., Lib X-Y., Liu G., Zeng E.Y., and Wang F., 2016 'Accuracy and application of quantitative X-ray diffraction on the precipitation of struvite product'. Water Res., 90, 9-14.

37. USEPA, 1991. 'A geochemical assessment model for environmental systems': Version 3.0 user manual. U.S. EPA. EPA/600/3-91/021. Washington, DC.

38. Hill R.J., and Howard C.J., 1987 'Quantitative phase analysis from neutron powder diffraction data using the Rietveld method'. J. Appl. Crystallogr., 20, 467-474.

39. Rietveld H.M., 1969. 'A profile refinement method for nuclear and magnetic structures'. J. Appl. Crystallogr., 2, 65-71.

40. Winburn R.S., Grier D.G., McCarthy G.J., and Peterson R.B., 2000 'Rietveld quantitative X-ray diffraction analysis of NIST fly ash standard reference materials'. Powder Diffr., 15, 163-172.

41. Rodriguez-Carvajal J., 2005 'Program Fullprof.2k, version 3.30', Laboratoire Leon Brillouin, France, June 2005.

42. Caglioti G., Paoletti A., and Ricci F.P., 1958 'Choice of collimator for a crystal spectrometer for neutron diffraction'. Nucl. Instrum., 35, 223-228.

43. Bayuseno A.P., and Schmahl W.W., 2015 'Improved understanding of the pozzolanic behaviour of MSWI fly ash with $Ca(OH)_2$ solution'. Int. J. Environ. Waste Manage., 15 (1), 39-66.

44. Mahieux P.-Y., Aubert J.-E., Cyr M., Coutand M., and Husson B., 2010 'Quantitative mineralogical composition of complex mineral wastes –Contribution of the Rietveld method'. Waste Manage., 30, 378–388.

45. Mijangos F., Kamel M., Lesmes G., and Muraviev D.N., 2004 Synthesis of struvite by ion exchange isothermal supersaturation technique. React. Funct. Polym., 60, 151-161.

46. Ohlinger K.N., Young T.M., and Schroeder E.D., 2000 'Postdigestion struvite precipitation using a fluidized bed reactor'. J. Environ. Eng., 126, 361-368.

47. Prince E., 1993. 'Mathematical aspects of Rietveld refinement'. The Rietveld Method. Edited by Young, R.A. International Union of Crystallography, Oxford, New York, 43-54.

48. Korchef A., Saidou H., and Ben Amor M., 2011 'Phosphate recovery through struvite precipitation by CO_2 removal: Effect of magnesium, phosphate and ammonium concentrations'. J. Hazard. Mater., 186, 602-613.

49. Ronteltap M., Maurer M., and Gujer W., 2007 'Struvite precipitation thermodynamics in source-separated urine'. Water Res., 41, 977-984.

50. Wilsenach J., Schuurbiers C., and van Loosdrecht M.C.M., 2007 'Phosphate and potassium recovery from source separated urine through struvite precipitation'. Water Res., 41, 458-466.

51. Prywer J., and Olszynski M., 2013 'Influence of disodium EDTA on the nucleation and growth of struvite and carbonate apatite'. J. Cryst. Growth, 375, 108-114.

52. Abbona F., and Boistelle R., 1979 'Growth morphology and crystal habit of struvite crystals ($MgNH_4PO_4 \cdot 6H_2O$)'. J. Cryst. Growth, 46 (79), 339-354.

53. Stratful I., Scrimshaw M.D., and Lester J.N., 2001 'Conditions influencing precipitation of magnesium ammonium phosphate'. Water Res., 35, 4191-4199.

54. Demeestere K., Smet E., Van Langenhove H., and Galbacs Z., 2001 Optimalisation of magnesium ammonium phosphate precipitation and its applicability to the removal of ammonium. Environ. Technol., 22 (12), 1419-1428.

55. Santinelli M., Eusebi A.L., Santini M., and Battistoni P., 2013 'Struvite crystallization for anaerobic digested supernatants: Influence on the ammonia efficiency of the process variables and the chemicals dosage modality'. Chem. Eng. T., 32, 2047-2052.

56. Ott H., 1926 'Die Strukturen von Mn O, Mn S, Ag F, Ni S, Sn I_4, Sr Cl_2, Ba F_2, praezisionsmessungen einiger alkalihalogenide'. Z. Kristallogr., 63, 222-230.

57. Whitaker A., and Jeffery J.W., 1970 'The crystal structure of struvite, $MgNH_4PO_4 \cdot 6H_2O$'. Acta Crystallogr. B26, 1429-1440.

Mineral speciation determination and quantitative x-ray analysis of struvite family crystals precipitated in wastewater

ORIGINALITY REPORT

19%	20%	9%	5%
SIMILARITY INDEX	INTERNET SOURCES	PUBLICATIONS	STUDENT PAPERS

PRIMARY SOURCES

1	eprints.undip.ac.id Internet Source	14%
2	hdl.handle.net Internet Source	2%
3	Submitted to Universitas Negeri Surabaya The State University of Surabaya Student Paper	2%

Exclude quotes	On	Exclude matches	< 2%
Exclude bibliography	On		

Mineral speciation determination and quantitative x-ray analysis of struvite family crystals precipitated in wastewater

GRADEMARK REPORT

FINAL GRADE

/0

GENERAL COMMENTS

Instructor

PAGE 1

PAGE 2

PAGE 3

PAGE 4

PAGE 5

PAGE 6

PAGE 7

PAGE 8

PAGE 9

PAGE 10

PAGE 11

PAGE 12

PAGE 13

PAGE 14

PAGE 15

PAGE 16

PAGE 17

PAGE 18

PAGE 19

PAGE 20

PAGE 21

PAGE 22

PAGE 23